



Designing standalone hybrid energy systems minimizing initial investment, life cycle cost and pollutant emission



A.T.D. Perera, R.A. Attalage*, K.K.C.K. Perera, V.P.C. Dassanayake

Department of Mechanical Engineering, Faculty of Engineering, University of Moratuwa, Moratuwa 10400, Sri Lanka

ARTICLE INFO

Article history:

Received 17 September 2012
Received in revised form
12 January 2013
Accepted 5 March 2013
Available online 9 April 2013

Keywords:

Hybrid energy systems
Standalone applications
Multi-objective optimization
Life cycle cost
GHG (Green House Gas) emission
Initial investment

ABSTRACT

HES (hybrid energy system)s are becoming energy systems of choice for standalone applications due to ever increasing fuel costs and global concern on GHG (Green House Gas) emissions. However, it is difficult to justify the higher ICC (Initial Capital Cost) of renewable energy components, especially for rural electrification projects in developing countries. This paper illustrates the modeling and simulation of HESs, and multi-objective optimization carried out in order to support decision-making in such instances. LEC (Levelized Energy Cost), ICC and GHG emission were taken as objective functions in the optimization and the sensitivity of market prices and power supply reliability was further evaluated. Results depict that Pareto front of LEC, ICC and GHG emission can be simplified as a combination of ICC–LEC and LEC–GHG emission Pareto fronts making the decision-making process simpler. Gradual integration of renewable energy sources in a number of design stages is proposed for instances where it is difficult to bear the higher ICC. Finally, importance of planning integration of renewable energy sources at early design stages of the project is highlighted in order to overcome the difficulties that need to be faced when coming up with the optimum design.

Crown Copyright © 2013 Published by Elsevier Ltd. All rights reserved.

1. Introduction

HES (hybrid energy system)s are becoming popular for off grid electrification as many applications around the world are reported [1–6]. HESs are economical, consume less fossil fuels, and produce less GHG (Green House Gases) [3,7]. Due to these advantages modeling, simulation, and optimization of off grid HESs have become an area of interest during the last few years [8,9].

Determining optimum system configuration and operation strategy becomes important at the early design stages of HESs [10]. This is a challenging process due to the complexity of decision space variables and objective functions. Several optimizing algorithms based on, numerical [11,12], probabilistic [13] and heuristic [14–16] techniques have been proposed to derive the optimum design. Furthermore, conflicting objectives such as cost, unmet load fraction, pollutant emission and utilization efficiency of renewable energy have been taken into consideration through multi-objective optimization [17–21]. Previous literature on multi-objective optimization of HESs have been reviewed by Fadaee and Radzi [22] and highlighted the importance of adapting the optimization process in order to match with the local context.

HESs are currently used in Sri Lanka to supply the power requirement of telecommunication towers and proposed for rural electrification projects far away from the existing power grid. Higher ICC (Initial Capital Cost), fuel transportation and maintenance of the ICG (Internal Combustion Generator) can be taken as the main challenges that need to be overcome when designing standalone HESs in developing countries [7,23]. At the same time, it is important to evaluate the sensitivity of fuel prices and the cost of renewable energy components (i.e. wind turbines and solar panels) on optimum design due to present market volatility. Reliability of power supply needs to be assured which plays a major role when developing the final design. Therefore, it is important to identify the best practices that can be adopted while evaluating all the above aspects through multi-objective optimization, which is taken into discussion in this work for a rural electrification project.

Designers try to minimize the ICC and the LEC (Levelized Energy Cost) at early design stages of HESs considering financial limitations. At the same time, it is expected to minimize the fuel consumption and the GHG emission considering environmental impact and fuel transpiration. However, it is essential to bear a higher ICC when it comes to renewable energy sources although the operational and maintenance costs are low. On the other hand, the ICC required for the ICG is quite small compared to the operational and maintenance cost. When it comes to life cycle cost, it has been shown that optimum selection of renewable energy sources along with dispatchable energy sources can reduce the life cycle cost of HESs when

* Corresponding author. Tel.: +94 714964961; fax: +94 112650621.

E-mail addresses: dinu@mech.mrt.ac.lk, raattalage@gmail.com (R.A. Attalage).

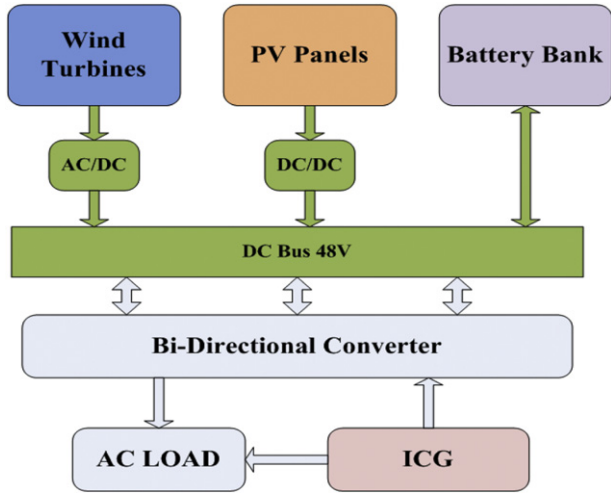


Fig. 1. HES configuration.

compared to ICG systems [3,7]. Therefore, the LEC and the ICC become conflicting objectives resulting in a Pareto front. Similarly, the LEC and the GHG emission (or fuel consumption) produce a Pareto front as they also conflict with each other [18,20,24]. Therefore, it is important to analyze the Pareto front of ICC–LEC–GHG emission considering the impact of power supply reliability and current market changes in fuel price and renewable energy sources. Finally, it is important to develop innovative methods to overcome techno-economical challenges when designing HESs. A concise description on the modeling and simulation techniques used in this work is given in Sections 2 and 3 respectively. Section 4 illustrates the optimization technique used, decision space variables and objective functions. Finally, the results are analyzed in Section 5.

2. Mathematical model developed

A HES consisting of wind turbines, SPV (Solar PV) panels, ICG, AC (alternative current)–DC (direct current), DC–AC converters, battery bank and a battery charger is taken into consideration in this work (Fig. 1).

2.1. Energy flow through SPV panels

Hourly solar irradiation on the tilted SPV panel and the energy conversion efficiency of the modules need to be modeled in order to estimate the power output from SPV panels. Hourly horizontal solar irradiation data is used to compute hourly tilted solar irradiation (G_{β}) values using Klucher [25] and Climed-2 models [26]. The semi-empirical formula proposed by Durisch et al. [27] is used to compute the efficiency of SPV panels (η_{pv}) according to Eq. (1).

Table 1
Parameters for the SPV efficiency model for different solar panel types.

	p	q	r	s	m	u
Monocrystalline	23.62	-0.2983	-0.09307	-0.9795	0.1912	0.9865
Polycrystalline	15.39	-0.1770	-0.09736	-0.8998	0.0794	0.9324
Amorphous	36.02	-0.7576	-0.02863	-1.1432	0.6601	1.0322

$$\eta_{pv} = p \left[q \frac{G_{\beta}}{G_{\beta,0}} + \left(\frac{G_{\beta}}{G_{\beta,0}} \right)^m \right] \cdot \left[1 + r \frac{\theta_{cell}}{\theta_{cell,0}} + s \frac{AM}{AM_0} + \left(\frac{AM}{AM_0} \right)^u \right] \quad (1)$$

In Eq. (1), AM denotes the air mass value [28] and θ_{cell} is the cell temperature. The following values are used: $G_{\beta,0} = 1000 \text{ W m}^{-2}$, $\theta_{cell,0} = 25 \text{ }^{\circ}\text{C}$ and $AM_0 = 1.5$. Parameters p, q, r, s, m, u for different SPV technologies are taken from Table 1 [27,29].

Hourly power output from the SPV panels ($P_{SPV}(t)$) is calculated using Eq. (2). Minor losses taken place in the energy conversion, including efficiency drop at the inverter, dust accumulation on SPV panels etc are taken into account through η_{C-SPV} .

$$P_{SPV}(t) = G_{\beta}(t) \eta_{pv}(t) A N_{SPV} \eta_{C-SPV} \quad (2)$$

2.2. Energy flow through wind turbines

Power law approximation (Eq. (3)) is used to compute wind speed at wind turbine hub level, based on wind speed data collected at an anemometer height of 12 m.

$$V_{hub}(t)/V_{ane}(t) = (Z_{hub}/Z_{ane})^{\gamma} \quad (3)$$

In Eq. (3), $V_{hub}(t)$ and $V_{ane}(t)$ are wind speeds at hub level (Z_{hub}) and anemometer height (Z_{ane}), γ denotes the power law exponent taken as 0.14.

Several mathematical models have been introduced to model the power output from wind turbines. These models can be divided into two major categories, i.e. mathematical models based on power available in wind and conceptual power curve of wind turbines. The latter can be further sub-divided to mathematical models based on presumed shape of power curve and actual power curve of wind turbine [30]. Thapar et al. [30] show that a mathematical model based on the actual power curve of a wind turbine provides a much more accurate result compared to other techniques. Therefore, cubic spline interpolation technique [31,32], which is a method based on the actual power curve of the wind turbine is used in this work, to model the power output of turbines. The power curve provided by the manufacturer of a locally available wind turbine is used and the power curve of the wind turbine is modeled by using n_s number of cubic spline interpolation functions, considering $n_s + 1$ points from the power curve given by the manufacturer (Eq. (4)).

$$\tilde{P}_w(t) = \begin{cases} \tilde{P}_w = 0, & V_{hub}(t) < V_{ci} \\ \tilde{P}_w = a_1 V_{hub}^3 + b_1 V_{hub}^2 + c_1 V_{hub} + d_1, & V_{ci} < V_{hub}(t) < V_1 \\ \tilde{P}_w = a_2 V_{hub}^3 + b_2 V_{hub}^2 + c_2 V_{hub} + d_2, & V_1 < V_{hub}(t) < V_2 \\ \dots & \dots \\ \tilde{P}_w = a_{n_s} V_{hub}^3 + b_{n_s} V_{hub}^2 + c_{n_s} V_{hub} + d_{n_s}, & V_{n_s-1} < V_{hub}(t) < V_r \\ \tilde{P}_w = P_r, & V_r < V_{hub}(t) < V_{co} \\ \tilde{P}_w = 0, & V_{co} < V_{hub}(t) \end{cases} \quad (4)$$

In Eq. (4), a_i , b_i , c_i , and d_i represent coefficients of the polynomial function which vary with the power curve of the wind turbine. Further, V_r , V_{ci} , a , V_{co} and P_r denote the rated wind speed, cut-in wind speed, cut-off wind speed and rated power of the wind turbine respectively.

Finally, the electric power from the wind turbines is calculated according to Eq. (5)

$$P_w(t) = \tilde{P}_w(t) N_w \eta_{w-inv} \quad (5)$$

where N_w denotes the number of wind turbines and η_{w-inv} denotes inverter efficiency.

2.3. Mathematical model for the battery bank

SOC (State of Charge) model [33] was used to compute the charge level of the battery bank. Rain Flow Algorithm based on Downing's Algorithm [34,35] was used to compute the lifetime of the battery bank.

2.4. Fuel consumption of the ICG

The hourly power requirement from the ICG is determined through the Combined Dispatch Strategy (illustrated in Section 3). Load factor of the ICG is determined based on the Dispatch Strategy, and used to calculate $FC(t)$ (hourly fuel consumption) from ICG. In most of the instances, the fuel consumption was assumed to vary linearly with the load factor [36,37]. The fuel consumption is taken as a polynomial function of the load factor in this work, considering the nonlinear components of the fuel curve (Fig. 2). A detailed description about the energy flow model can be found in Ref. [38].

2.5. Life cycle cost model

Several life cycle cost models have been proposed to analyze the cash flow of HESs [39–42]. A simple life cycle cost model is developed in this work based on previous publications of Kaldellis et al. [41] and Diaf et al. [39], which is illustrated in detail in this section.

LCC (life cycle cost) of the system consists of two components i.e. ICC and OM cost (Operation and Maintenance). ICC of system components comprises the AC (acquisition costs) and the installation costs. Installation cost of system components is taken as a fraction of AC (α) (Table 2) (Eq. (6)).

$$ICC = (1 + \alpha)AC \quad (6)$$

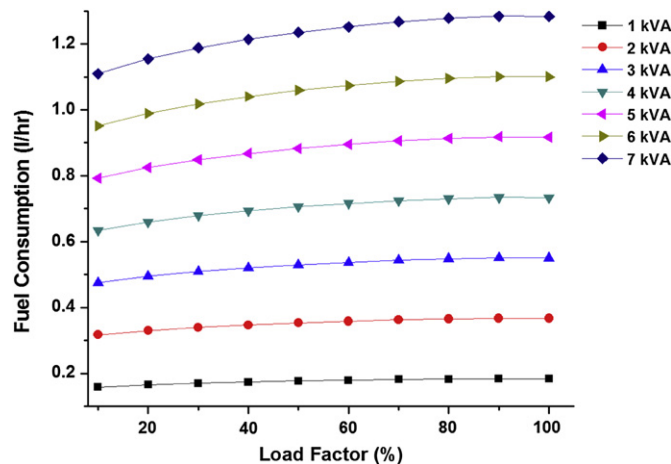


Fig. 2. Variation of fuel consumption with load factor.

ICC of the system (ICC_0) is calculated considering the initial expenditure on ICG (ICC_{Gen}), wind turbines (ICC_W), SPV panels (ICC_{SPV}), battery bank (ICC_B) and inverters (ICC_{Inv}) according to Eq. (7).

$$ICC_0 = ICC_{Gen} + ICC_W + ICC_{SPV} + ICC_B + ICC_{Inv} \quad (7)$$

When it comes to OM, it comprises FOM (Fixed OM) and VOM (Variable OM) cash flows. The annual fuel consumption cost, and the maintenance cost for the ICG, wind turbines and SPV panels are taken into consider under FOM expenditure.

Eq. (8) is used to compute the PV (Present Value) of entire FOM cash flows (FOM_{PV}), where CRF denotes the Capital Recovery Factor, which is computed using Eq. (9). In Eq. (9), p denotes the annual real interest rate, and n denotes the lifetime of the project in years. Annual real interest rate p is finally calculated using Eq. (10) where f and g denote return on investment and local market annual inflation rate (Table 2).

$$FOM_{PV} = FOM.CRF \quad (8)$$

$$CRF = (p(1 - p^n))/(1 - p) \quad (9)$$

$$p = (1 + f)/(1 + g) \quad (10)$$

VOM includes replacement cost of battery bank, ICG and inverters, which depends on operating conditions, number of operating hours and life expectancy. It is assumed that both SPV panels and wind turbines are having the exact lifetime of the project. Finally, the Present Value of the entire VOM cash flows (VOM_{PV}) is calculated using Eq. (11) considering the Present Value of VOM of each year.

$$VOM_{PV} = \sum_{k=1}^{k=n} p^k VOM_k \quad (11)$$

The NPV (Net Present Value) of the LCC comprises ICC_0 , FOM_{PV} and VOM_{PV} , which is used to calculate the LEC according to Eq. (12) where ELD (Electricity Load Demand) denotes the hourly electricity load demand.

$$LEC = LCC / \sum_{k=1}^{k=n} \sum_{t=1}^{t=8760} ELD_{t,k} \quad (12)$$

Local market prices of the system components are given in Tables 2 and 3.

2.6. Mathematical model for pollutant emission

Combustion of fossil fuels in ICGs release a number of noxious gases including CO, NO_x , SO_x and PM (Particulate Matter) etc. Hourly emission rates of various exhaust gases depend upon dynamic load factor of the ICG, engine technology and manufacturer [43]. However, total amount of CO_2 produced has been used along with fuel consumption or energy produced through the ICG in previous publications, neglecting the sensitivity of load factor of the

Table 2
Parameters of the cost model.

Parameter	Percentage (%)
SPV panel & wind turbines	
Installation cost as a fraction of acquisition cost	20
Annual O&M as a fraction of acquisition cost	5
ICG installation cost as a fraction of acquisition cost	5
Local market annual inflation rate	2

Table 3
Present local market prices system components.

Component	Description	Cost (\$)
Wind turbine	1 kW	2081
	5 kW	9588
Solar panels including inverters and ground mounting structure	Monocrystalline (1.22 m ²)	888
	Polycrystalline (0.79 m ²)	945
	Amorphous (1.28 m ²)	877
Single phase ICG (20,000 working hours)	0.5 kVA–7.5 kVA	335.5–4195
	Hourly O&M	0.11
Cost of fuel (Diesel 1 L)		1.03
Battery Bank	12 V, 250 Ahs × 4	500 × 4

ICG on emission [18,20,24]. As a result, impact of dispatch strategy on the GHG emission has not been depicted in the emission model. Moreover, impact of pollutants such as CO, NO_x, SO_x and PM (Particulate Matter) etc. has not been evaluated. In order to rectify the above issues, dynamic emission model based on the load factor of the ICG is introduced in the present study. Emission rates of CO, NO_x, SO_x and PM were taken for different load factors of the ICG [44] (i.e. 10%, 25%, 75% and 100% given in Table 4), and Lagrangian interpolation is used to calculate the hourly exhaust emissions. Finally, the Eq. CO₂ model introduced by Lora & Salomon [45] is used to compute the ecological and environmental impact of noxious gasses (taken as GHG emission).

3. Simulation of HES

The simulation combines hourly varying meteorological data and the ELD according to the operation strategy designed by the system designer known as the dispatch strategy. Time series of hourly wind speed and solar irradiation data are taken and the renewable energy output is computed by using the mathematical model illustrated in Section 2. When the renewable energy potential is not sufficient to provide the power requirement, dispatchable energy sources are used. Detailed description about the control strategy and brief description about the time series of hourly wind speed, solar irradiation and ELD are illustrated in this section.

3.1. Meteorological data and ELD (Electricity Load Demand)

Hourly average wind speed and solar irradiation values of 1995, 1997 and 1998 at Hambanthota, a southeast location of Sri Lanka (06°07' N 81°07' E) are taken in this study. When it comes to ELD, it is highly specific to the application. In this study, the ELD is considered to vary with the summer-weekly load variation proposed by IEEE (Institute of Electrical and Electronics Engineers) system reliability committee [46] (Fig. 3).

3.2. Dispatch Strategy

Combined Dispatch Strategy, which is a combination of Battery Charging Strategy, Frugal Discharge Strategy, SOC Set Point Strategy, Load Following Strategy, and Peak Shaving Strategies used in

Table 4
Average emission rates of various exhaust gases under different generator load conditions.

Generator load percentage	THC g/kWh	CO g/kWh	NO _x g/kWh	PM g/kWh	CO ₂ g/kWh
10	5.6	32	43	1.1	1487.94
25	6.8	23	38	1.2	970.44
50	2.5	15	37	1.9	793.17
75	13	10	29	2.6	736.67
100	15	09	26	2.1	727.22

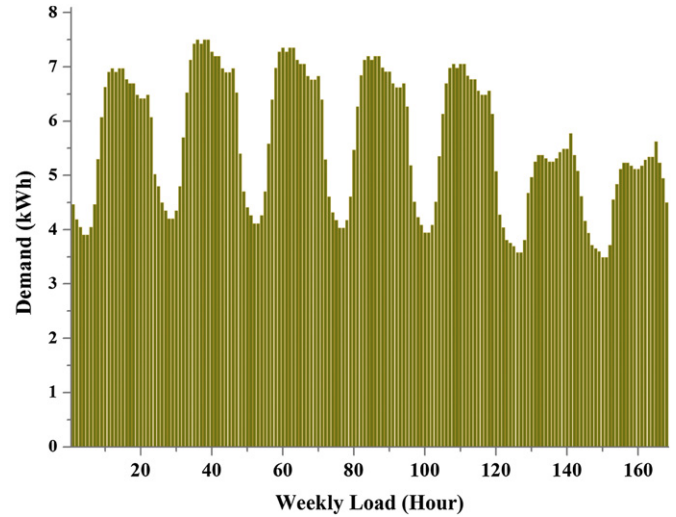


Fig. 3. Hourly variation of ELD.

this work [10,36,37] (Fig. 4). Detail description about the Dispatch Strategy is illustrated in this section.

3.2.1. State 1: Battery Charging Strategy

When electricity production through renewable energy sources, $P_R(t)$ ($P_w(t) + P_{SPV}$) is higher than the ELD, additional energy produced is used to charge the battery bank. However, when the battery bank reaches its maximum SOC, additional energy produced will be wasted, which is known as the WRE (Wasted Renewable Energy). The Battery Charging Strategy is quite easy to understand since it does not take any support from the dispatchable energy sources to supply the power requirement.

3.2.2. State 2: Frugal Discharge Strategy

Dispatchable energy sources are used to supply the additional power requirement when the power output from the renewable energy sources is inadequate. When the requirement of the dispatchable energy i.e. difference between ELD and $P_R(t)$ (P_a) is small, it is not advisable to use the ICG to provide the additional power requirement which will result in poor efficiency and higher OM cost. Therefore, the battery bank is used in such instances to supply the additional power until it reaches P_D (dispatch load), which is optimized in the optimization algorithm.

3.2.3. State 3: SOC Set Point Strategy

When the additional power requirement goes beyond P_D (dispatch load) the system will shift to SOC Set Point Strategy where the ICG is driven at its maximum power (P_{ngen}) and the additional power produced is used to charge the battery bank till it gets into set point SOC ($SOC_{set\ point}$) which is optimized using optimization algorithm.

3.2.4. State 4: Load Following Strategy

Additional conversion losses will take place when the battery bank is charged using the ICG. At the same time, this will minimize the renewable energy storage capacity. Therefore, when P_a is greater than (critical load) the system will shift to Load Following Strategy where the ICG is driven to supply P_a and battery will not take place. P_C is also optimized in the optimization algorithm.

3.2.5. State 5: Peak Shaving Strategy

When the additional power required goes beyond P_{ngen} , Peak Shaving Strategy is used where the battery bank will be used to along with the ICG.

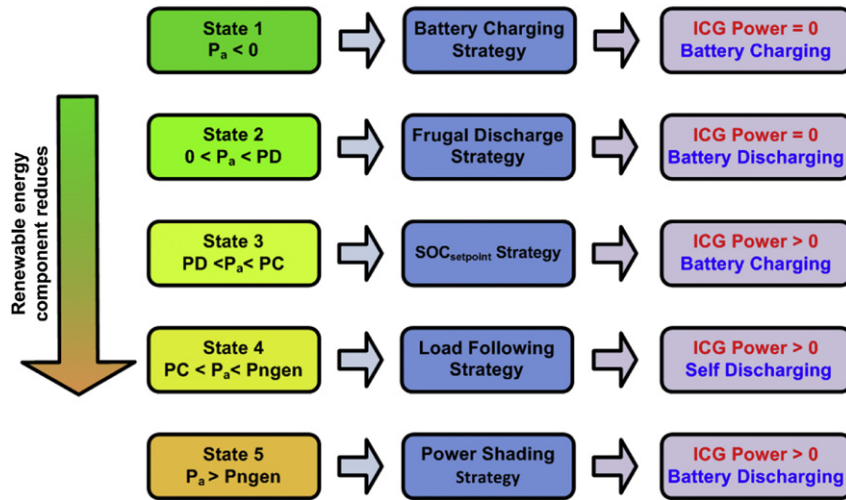


Fig. 4. Dispatch strategy.

3.3. Breakdown of power supply

The power supply breakdowns when $P_a(t)$ is greater than the addition of P_{ngen} and the maximum power output of the battery bank ($P_{Bat-Max}$). Loss of Power Supply ($LPS(t)$) can be calculated using Eq. (13)

$$LPS(t) = P_a(t) - P_{ngen} - P_{Bat-Max} \quad (13)$$

Finally, the unmet load fraction is calculated using Eq. (14) which is taken as the measure of power supply reliability.

$$\text{Unmet load fraction} = \frac{\sum_{t=1}^{t=8760} LPS(t)}{\sum_{t=1}^{t=8760} ELD(t)} \quad (14)$$

4. Multi-objective optimization of HES

It is a challenging process to come-up with the optimum system configuration and the operation strategy when designing HESs. Objective functions related to the problem are neither linear nor analytical. At the same time, some of the decision space variables are continuous while some are discrete. Therefore, enumerative and heuristic methods become more appropriate compared to classical gradient based techniques. A number of enumerative algorithms have been developed in order to optimize HESs during the last few years [12,47–49]. Furthermore, software based on enumerative techniques such as HOMER has been used extensively in order to come-up with the optimum system design [1,3,50,51]. However, when compared to heuristic methods, computational time required to obtain the optimum solution is much higher when it comes to enumerative techniques [50]. As a result of this, recent reviews on HES optimization highlight the importance of using heuristic techniques in order to optimize HESs [22,52]. A number of heuristic techniques including Genetic Algorithm [14,36,53], Simulated Annealing [16], Particle Swarm method [15,54] etc. were used to develop algorithms to optimize HESs. Furthermore, evolutionary algorithms were used to carry out multi-objective optimizations considering conflicting objectives.

4.1. Optimization algorithm

Considering these perspectives, Steady ϵ -State Evolutionary Algorithm [55], based on the ϵ -dominance technique [56], is used in

this study to come-up with Pareto fronts considering conflicting objectives. Initial population is randomly generated in the optimization algorithm and objective function values are computed after the life cycle simulation (Fig. 5). Based on objective function values,

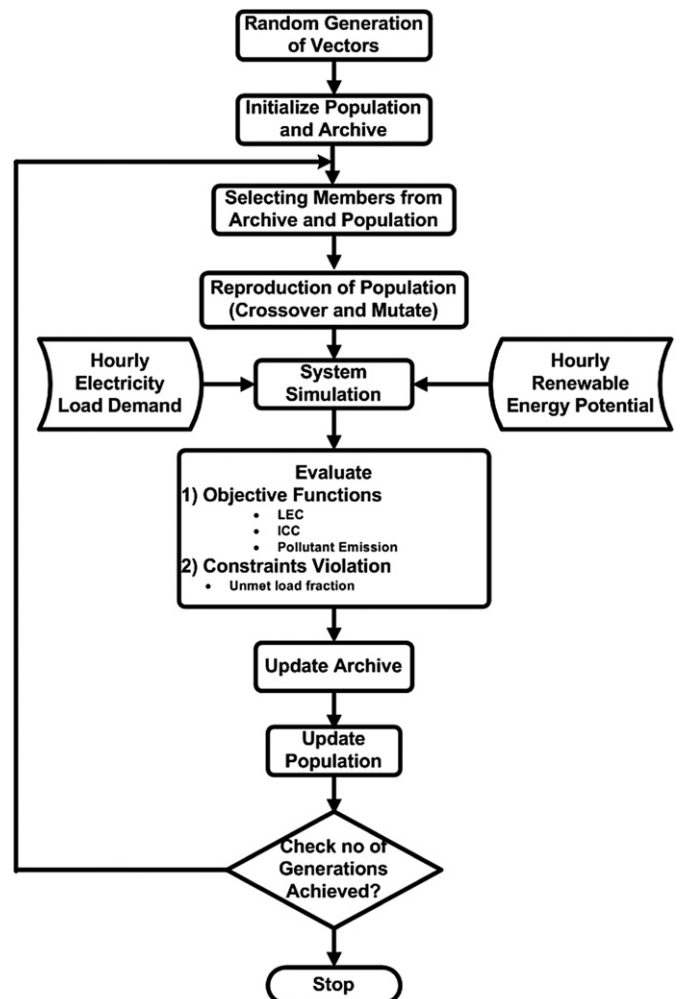


Fig. 5. Optimization algorithm.

Table 5
Range of decision space variables.

Variable	Minimum	Maximum	Interval	Discrete/Continuous
SPV type	0	3	1	Discrete
SPV panels	0	220	1	Discrete
Wind turbine power	0	2	1	Discrete
Wind Turbines	0	20	1	Discrete
No of batteries	0	100	4	Discrete
ICG capacity (kVA)	0	7.5	0.5	Discrete
SOC _{min}	30%	50%	–	Continuous
P _{min}	30%	50%	–	Continuous
SOC _{set_value}	70%	100%	–	Continuous
P _d	P _{min}	P _{ngen}	–	Continuous

a non-dominant set of alternative solutions are selected which produces the initial archive. After coming up with the initial archive and the population, both crossover and mutation operators are used along with the constraint tournament method to reproduce the population and archive. This routine takes place until the termination of main loop, which occurs when desired generations were achieved.

4.2. Operators used in the optimization algorithm

Some of the decision space variables of the optimization problem are continues while some are discrete. Hence, real parameter operators; Simulated Binary Crossover Operator [57] and Polynomial Mutation Operator [58] were used in this study instead of binary coded operators.

4.3. Decision space variables and objective functions

System configuration parameters that relate with the dispatchable, non- dispatchable energy sources and the storage were optimized using the optimization algorithm. The upper and lower bounds of these variables are selected according to Table 5. Similarly, the variables related with the operation strategy were optimized. Operation of the ICG is controlled through three main parameters, P_D, P_C and P_{min} (illustrated in Section 3.3). The upper and lower bounds of these variables were selected according to Table 5. Other parameters related with the dispatch strategy such as SOC_{min} and SOC_{set-value} were optimized simultaneously (Table 5). Objective functions derived in Sections 2 and 3 were used in the optimization algorithm. A detailed description about the objective functions and constraints used for different optimization problems is given in Table 6.

Table 6
Objective functions and constraint used in different optimization problems.

No of objectives	Objectives	Constraint unmet load fraction (%)	Sensitivity
3	LEC, ICC ₀ , emission equivalent	2, 5, 10	Unmet fraction (2%, 5%, 10%)
2	LEC–ICC ₀	2	Fuel cost (present price, +5%, +10%, +15%)
2	LEC–ICC ₀	2	Wind turbine and SPV panel cost (present price, –5%, –10%)
2	LEC–emission equivalent	2	Fuel cost (present price, +5%, +10%)
2	LEC–emission equivalent	2	Wind turbine and SPV panel cost (present price, –5%, –10%)

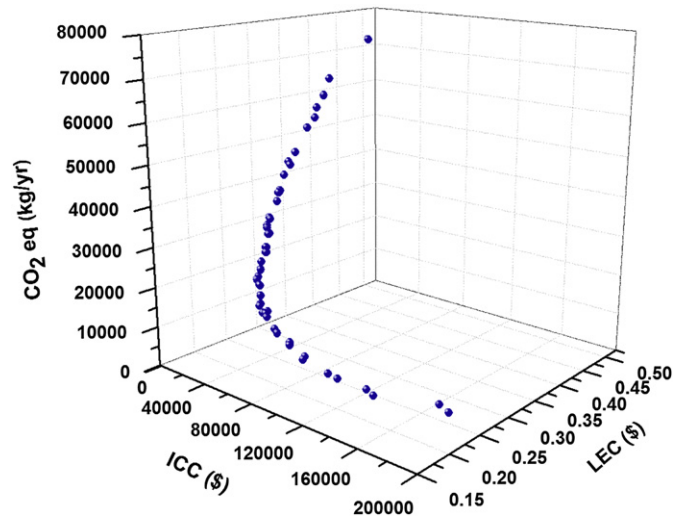


Fig. 6. Pareto front of ICC, LEC and GHG emission with unmet load fraction of 2%.

5. Results and discussion

Obtained results from the multi-objective optimization considering several sets of objectives are taken into discussion in this section.

5.1. Pareto optimization of ICC, LEC and GHG emission

Pareto front of ICC–LEC–GHG emission (or fuel consumption) portrays a better picture of the alternative design solutions that need to be evaluated when coming up with the final design. GHG emission is taken to represent both fuel consumption and GHG emission instead of taking these aspects as two separate objectives. Finally, Pareto fronts were taken for three different unmet load fractions i.e. 2%, 5% and 10% (Figs. 6–8).

When analyzing these three Pareto fronts, it was observed that the LEC reduces with the increase of ICC initially, and reaches to a minimum (Region A in Fig. 9). In Region A, both GHG emission and LEC become non-conflicting objectives since both of these functions decrease with the increase of ICC. Therefore, the solutions of this region do not appear in LEC–GHG emission Pareto

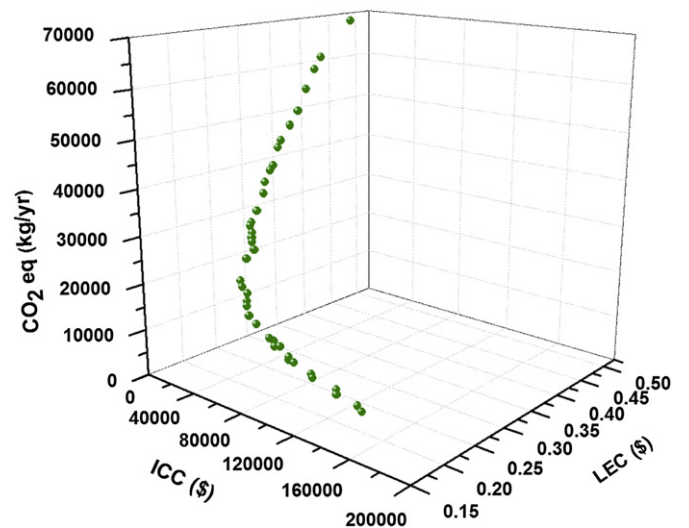


Fig. 7. Pareto front of ICC, LEC and GHG emission with unmet load fraction of 5%.

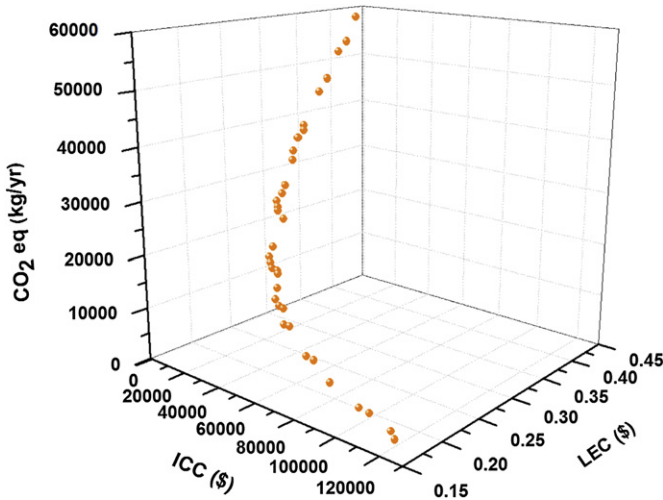


Fig. 8. Pareto front of ICC, LEC and GHG emission with unmet load fraction of 5%.

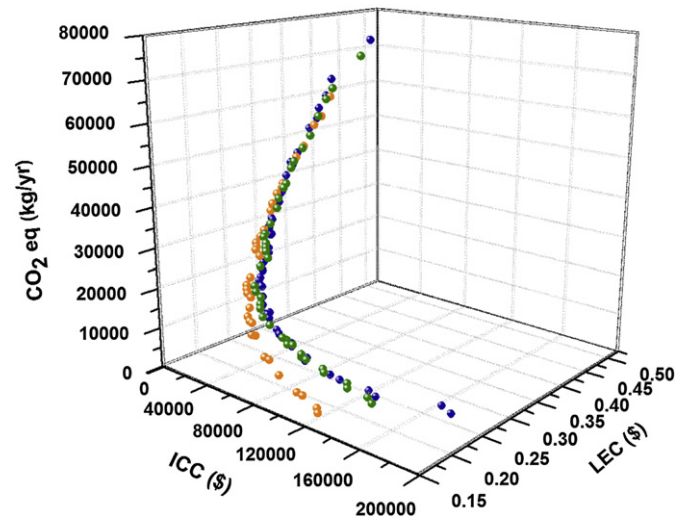


Fig. 10. Impact of power supply on ICC, LEC and GHG emission Pareto front.

front. With further reduction of GHG emission beyond the minimum LEC, both ICC and LEC vary parallel to each other (becomes non-conflicting) and get increase with the reduction of GHG emission (Region B). Therefore, Region B comes into the picture when taking LEC–GHG emission Pareto front. This makes it important to come-up with the system design which minimizes the LEC initially, and based on that, it can be determined whether to use LEC–GHG emission or LEC–ICC Pareto front while analyzing limitations of ICC, fuel transportation, GHG emission, maintenance of ICG etc.

5.2. Sensitivity of power supply reliability and market prices

Power supply reliability is having a notable impact on the design. Based on the Pareto fronts obtained, it can be interpreted that both GHG emission and ICC have increased with the increase of power supply reliability (Fig. 10). However, the sensitivity of unmet load fraction is insignificant when comparing 2%–5% unmet load fractions.

Due to highly volatile market conditions, sensitivity of market prices needs to be studied at early design stages. When it comes to

SPV panels, notable price reduction can be observed during recent past [60]. At the same time, Bolinger and Wiser [59] reveal that there is a reduction in wind turbine prices in present U.S. market. In order to estimate the impact of price reduction in SPV panels and wind turbines, LEC–ICC Pareto fronts were taken with 5% and 10% reduction of present market prices (Fig. 11). Further, sensitivity analysis was conducted for LEC–HG emission Pareto front (Fig. 12). When analyzing the Pareto fronts, it was observed that the impact of cost reduction in renewable energy components is not significant in ICC–LEC Pareto front, especially with lower ICCs. Dominant role of ICG can be taken as the reason behind this observation. However, the cost reduction makes a notable impact on LEC–GHG emission Pareto front with the increase of renewable energy fraction.

Escalation of fuel prices and its impact on the Pareto fronts are evaluated by taking into account 5%, 10% and 15% increase of the present market price of fuel. Although the sensitivity of fuel cost is insignificant on the ICC, notable increase in the LEC was observed with the increase of fuel prices, especially when LEC is above 0.30 \$ (Fig. 13). When analyzing the Pareto front of LEC–GHG emission, it

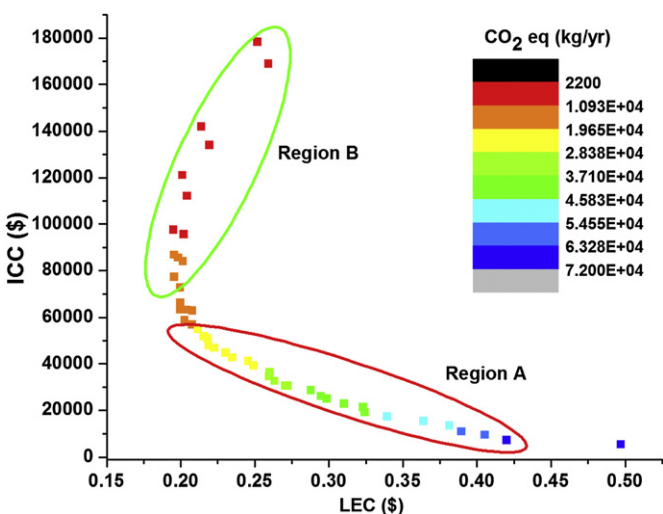


Fig. 9. Two main regions of ICC, LEC and GHG emission Pareto font with unmet load fraction of 2%.

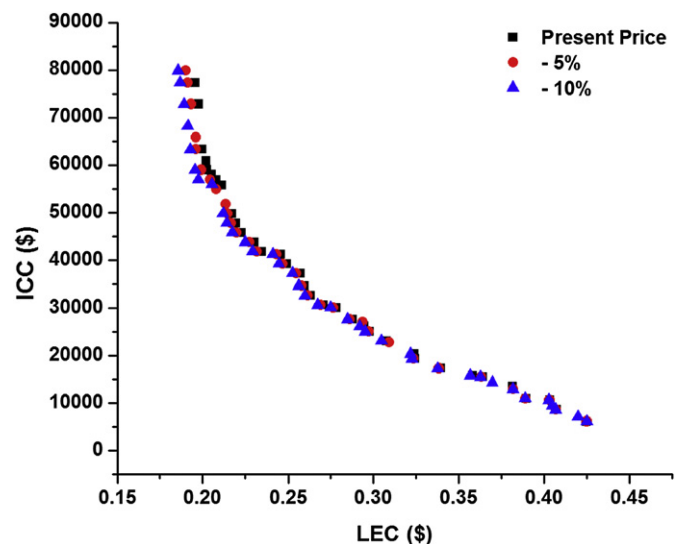


Fig. 11. ICC–LEC Pareto front with cumulative price reduction of SPV panels and wind turbines.

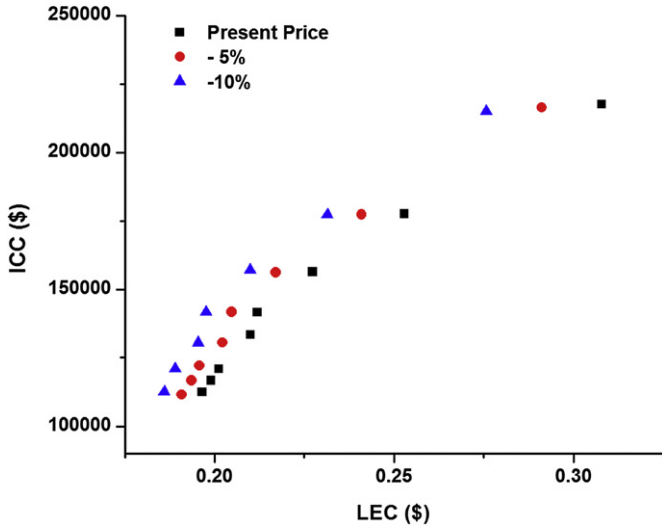


Fig. 12. Solutions of LEC-emission Pareto front with price reduction of renewable energy components.

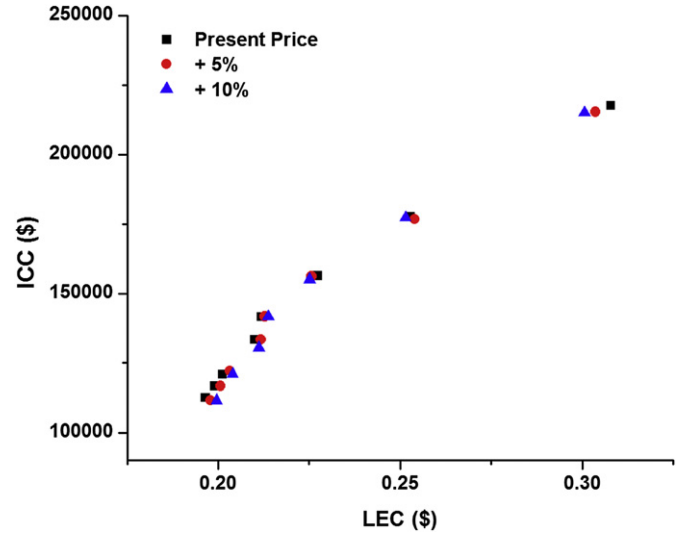


Fig. 14. ICC with LEC of solutions in LEC-emission Pareto front with increase of fuel prices.

was observed that the sensitivity of fuel escalation is insignificant (Fig. 14). When evaluating the sensitivity of both fuel prices and renewable energy sources, it is prudent that incorporating renewable energy sources beyond the minimum LEC (system designs in Region B) will help to overcome the vulnerability of the future fuel price escalation while taking advantage of cost reduction in renewable energy sources. Therefore, gradual integration of renewable energy sources in several stages needs to be encouraged when it is difficult to bear higher ICC.

5.3. Gradual integration of renewable energy sources

It is essential to come-up with an appropriate initial design for a project, which is to be extended later. The set of optimum design solutions of the Pareto front with unmet load fraction of 2% is taken into discussion in order to analyze the sequential process of adding renewable energy sources.

It is a challenging task to consider the entire Pareto front at once. Therefore, objective space is divided into six sections based

on the ICC, and several design solutions from each section are extracted and tabulated in Table 7. When analyzing these design solutions, it was observed that the LEC gradually reduces when moving from Section 1 to Section 5, and subsequently gets increased when moving to Section 6. Therefore, LEC–ICC Pareto front can be used to analyze the integration of renewable energy sources within Section 1 to Section 5. Pareto front of LEC–ICC–GHG emission needs to be taken when analyzing the cases that go up to Section 6. When considering the designs with lowest ICC (Section 1), ICG plays a dominant role, contributing almost 70% of the total power generation (Table 8). As a result of it, both fuel consumption and GHG emissions are quite high. When moving from Section 1 to Section 5, contribution of ICG gradually reduces while minimizing the fuel consumption and GHG emission (Tables 7 and 8). Gradual increase of battery bank is the other important feature that can be observed.

Selection of renewable energy sources in each step, is not that straight forward. When selecting 1-B as the initial design, renewable energy integration becomes quite simple. However, there are several limitations when selecting 1-A and 1-C as the initial design.

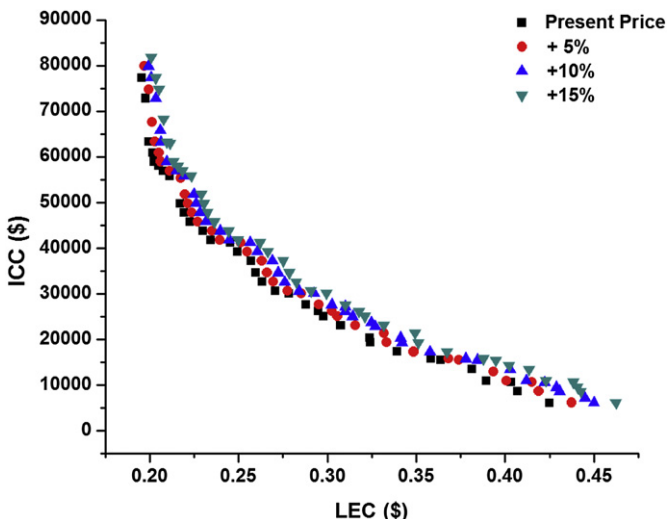


Fig. 13. ICC-LEC Pareto front with increase of fuel price.

Table 7

Selected set of solutions from ICC–LEC–GHG emission Pareto front.

Section- case	LEC (\$)	ICC (\$)	Emission (kg CO ₂ eq.)	Number of SPV panels ^a	Number of wind turbines	Number of battery banks	ICG capacity (kVA)
1-A	0.3639	15,475	52,436	0	3 ^b	2	6
1-B	0.3393	17,311	46,991	0	1 ^c	1	5.5
1-C	0.3237	20,363	45,006	1	1 ^c	2	5.5
2-C	0.2947	26,167	39,099	1	7 ^b	2	5
2-B	0.2708	30,640	34,070	0	2 ^c	2	5
3-A	0.2455	41,253	28,030	0	12 ^b	4	4.5
3-B	0.2344	41,794	25,850	0	3 ^c	2	4.5
4-B	0.2113	55,794	20,536	0	3 ^c	9	4.5
4-C1	0.2051	58,001	18,087	1	4 ^c	4	4
5-B	0.1956	77,336	13,721	0	5 ^c	8	5.5
5-C1	0.1946	81,094	13,185	1	5 ^c	9	7.5
5-C2	0.1991	116,706	8376	3	6 ^c	20	7.5
6-C1	0.2100	133,369	5927	6	7 ^c	21	7.5
6-C2	0.2273	156,382	3546	6	9 ^c	21	7.5

^a SPV panels with 'Amorphous' type.

^b Wind turbine with 1 kW capacity.

^c Wind turbine with 5 kW capacity.

Table 8
Fuel consumption and energy production of selected designs.

Section- case	Annual fuel consumption (l/yr)	Annual solar energy output (kWh/yr)	Annual wind energy output (kWh/yr)	Annual ICG energy output (kWh/yr)	Solar energy output (%)	Wind energy output (%)	ICG energy output (%)
1-A	12,145	0	9046	40,146	0	18	82
1-B	10,941	0	15,077	35,699	0	30	70
1-C	10,424	348	15,077	34,458	1	30	69
2-A	9056	348	21,108	29,935	1	41	58
2-B	7891	0	30,154	26,085	0	54	46
3-A	6492	0	36,185	21,460	0	63	37
3-B1	5987	0	45,231	19,791	0	70	30
4-A1	4757	0	45,231	15,722	0	74	26
4-B1	4189	348	60,308	13,847	0	81	19
5-B1	3178	0	75,385	10,504	0	88	12
5-C1	3054	348	75,385	10,095	0	88	12
5-C2	1940	1043	90,462	6413	1	92	7
6-C1	1373	2086	105,539	4538	2	94	4
6-C3	821	2086	135,693	2715	1	97	2

Since there are no design solutions with SPV panels with in Section 3, higher ICC is required when moving from Section 2 to Section 4 when starting with 1-C. At the same time, there is certain mismatch in wind turbine capacity when starting with 1-A. These two examples clearly depict that it is essential to plan the addition of renewable energy sources at each stage.

A possible path, that can be taken in the renewable energy integration process is taken into analysis in Fig. 15. This starts from 1-B and goes through 2-B, 3-B, 4-B1, 5-C1, up to 6-C2. Initial design comes up with a low ICC. Renewable energy sources are added gradually which reduces both fuel consumption and the

LEC in each step. When analyzing the sequential process, it was observed that fuel consumption gets reduced in each step at least by 20% and the LEC gets reduced at least by 8% (when considering the life cycle cost) in each step compared to the previous designs except in the final stage. In the final stage, the LEC gets increased by 14.4% compared to the previous stage although there is a significant reduction in the fuel consumption. Therefore, this design may not be economical in present context. However, with the reduction of costs in renewable energy components and escalating market prices of fossil fuels such systems may have financial feasibility in near future.

Rural electrification is been taken as the prime concern in this work. However, the obtained results through the analysis can be adapted for electrification of telecommunication towers, hotels and offshore lighthouses which are located close by to the location selected. It is essential to come-up with certain changes when moving towards other applications. Scale of the plant is having a notable impact on life cycle cost and need to be evaluated. Fuel transportation, becomes challenging for certain applications while power supply reliability becomes critically important for some other. Therefore, all the above factors need to be taken into evaluation in the decision-making process when moving to other applications.

Special attention needs to be given to the expansion of energy infrastructure, especially for rural electrification projects which is not taken into evaluation in this study. Furthermore, timeframe of each stage needs to be determined. This makes it important to move beyond the simple life cycle optimization of HESs and use a sequential optimization of the system considering each step while allowing for expansion of the grid which will be taken into consideration in future publications.

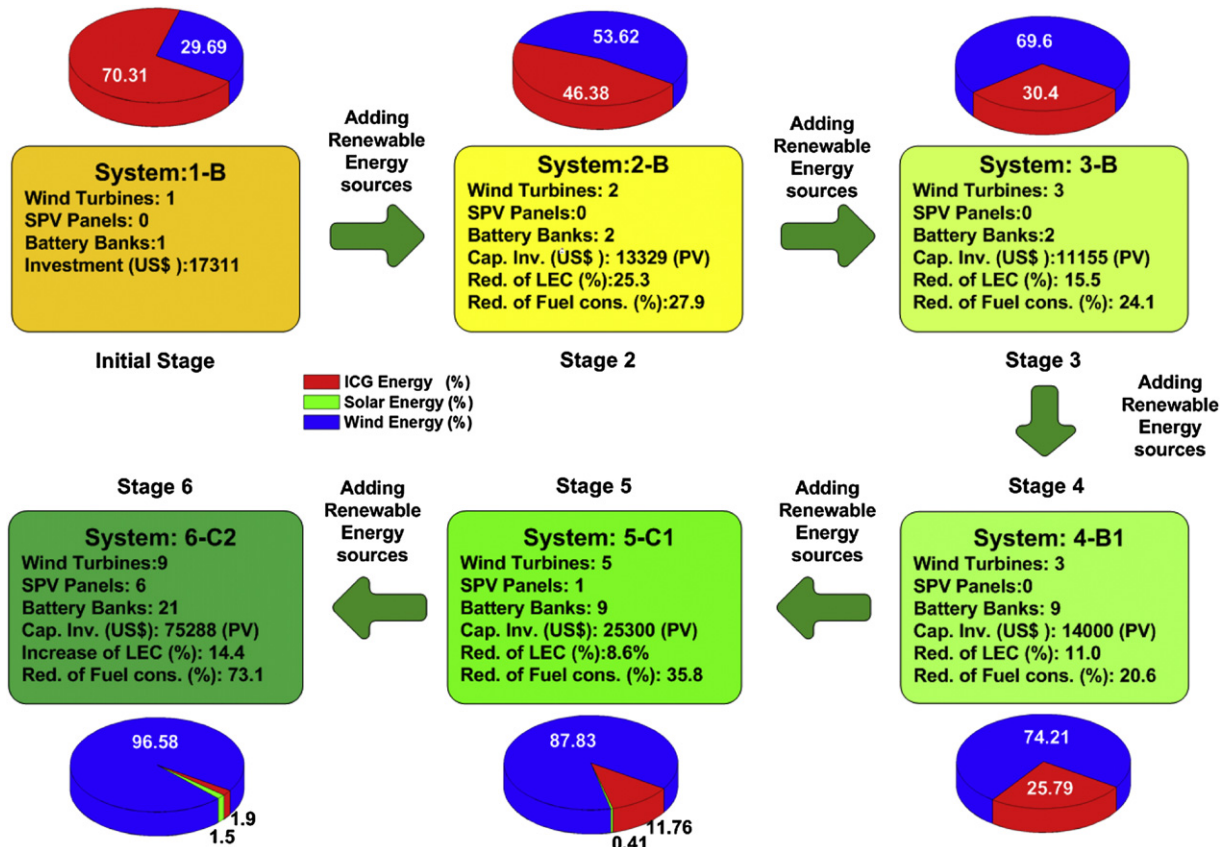


Fig. 15. Analysis of a complete renewable energy addition process.

6. Conclusion

It is essential to look over the possible methods of designing green energy systems in a viable manner. Set of alternatives obtained from multi-objective optimization considering LEC, ICC and emission provides a detail picture about the possible paths that can be taken in such circumstances. It is possible to simplify three dimensional Pareto front into two separate two dimensional Pareto fronts: ICC–LEC and LEC–GHG emission. Further, it was shown that power supply reliability is having a notable impact on the Pareto fronts. It was observed that ICC and GHG emission increase with the increase of power supply reliability.

When analyzing the sensitivity of present market conditions, it was found that fuel price escalation is having a significant impact on solutions in ICC–LEC Pareto front. At the same time, reduction of renewable energy component prices is having a positive impact on LEC-emission Pareto front. Therefore, gradual integration of renewable energy sources into HES becomes an attractive solution. However, it is essential to conduct a proper analysis when coming up with the initial system design and subsequent stages. An optimum pathway is analyzed in this work, which shows that both LEC, GHG emission and fuel consumption get reduce when going ahead. Therefore, gradual integration of renewable energy sources into existing HESs needs to be encouraged where it is difficult to bear higher ICC.

Acknowledgment

Authors would like to acknowledge Mr D.M.I.J. Wickremasinghe and Mr. D.V.S. Mahindaratna of University of Moratuwa for their help on developing the computer program. Further, the authors would like to thank Prof Ajith de Alwis from University of Moratuwa, Prof Saman Halgamuge and Dr Hans Gray from University of Melbourne and Nadeesh Madusanka from University of Cambridge for helping the group in various ways. This project is financially supported by a Senate Research Committee Grant–University of Moratuwa (SRC/LT/2011/12).

Nomenclature

α	power law exponent
β	tilt angle of SPV panel
η_{ch}	battery charging efficiency
η_{pv}	efficiency of the SPV panels
θ_a	ambient temperature
θ_{cell}	cell temperature
σ	hourly self-discharge coefficient
AM	air mass value
A_{SPV}	panel area
C_{Bat}	capacity of battery bank
CRF	Capital Recovery Factor
ELD	Electricity Load Demand
FOM	Fixed OM
FOM_{PV}	Present Value of FOM
G_{β}	hourly tilted solar irradiation
g	rate of local market annual inflation
GHG	Green House Gases
HES	hybrid energy system
ICC	Initial Capital Cost
ICG	Internal Combustion Generators
LCC	life cycle cost
LEC	Levelized Energy Cost
LPS	Loss of Power Supply
N_{SPV}	number of SPV panels
OM	Operation and Maintenance cost
$P_{Bat-Max}(t)$	maximum power of the battery bank

$P_{Gen}(t)$	ICG power output
P_{ngen}	nominal power of the generator
PM	Particulate Matter
P_r	rated power of wind turbine
$P_{SPV}(t)$	hourly power output of the SPV panels
SOC	State of Charge
SPV	Solar PV
THC	total hydrocarbon
V_{CO}	cut-off speed of wind turbine
V_r	rated wind speed of wind turbine
VOM	Variable OM
VOM_{PV}	Present Value of Variable OM
V_r	rated wind speed

References

- [1] Nandi SK, Ghosh HR. A wind–PV–battery hybrid power system at Sitakunda in Bangladesh. *Energy Policy* 2009;37:3659–64.
- [2] Kanase-Patil AB, Saini RP, Sharma MP. Integrated renewable energy systems for off grid rural electrification of remote area. *Renewable Energy* 2010;35:1342–9.
- [3] Kumar Nandi S, Ranjan Ghosh H. Techno-economical analysis of off-grid hybrid systems at Kutubdia Island, Bangladesh. *Energy Policy* 2010;38:976–80.
- [4] Kaldellis JK. Optimum hybrid photovoltaic-based solution for remote telecommunication stations. *Renewable Energy* 2010;35:2307–15.
- [5] Dalton GJ, Lockington DA, Baldock TE. Feasibility analysis of stand-alone renewable energy supply options for a large hotel. *Renewable Energy* 2008;33:1475–90.
- [6] Dalton GJ, Lockington DA, Baldock TE. Case study feasibility analysis of renewable energy supply options for small to medium-sized tourist accommodations. *Renewable Energy* 2009;34:1134–44.
- [7] Díaz P, Arias CA, Peña R, Sandoval D. FAR from the grid: a rural electrification field study. *Renewable Energy* 2010;35:2829–34.
- [8] Bernal-Agustín JL, Dufo-López R. Simulation and optimization of stand-alone hybrid renewable energy systems. *Renewable and Sustainable Energy Reviews* 2009;13:2111–8.
- [9] Zhou W, Lou C, Li Z, Lu L, Yang H. Current status of research on optimum sizing of stand-alone hybrid solar–wind power generation systems. *Applied Energy* 2010;87:380–9.
- [10] Gupta A, Saini RP, Sharma MP. Modelling of hybrid energy system—part II: combined dispatch strategies and solution algorithm. *Renewable Energy* 2011;36:466–73.
- [11] Kellogg W, Nehrir MH, Venkataramanan G, Gerez V. Optimal unit sizing for a hybrid wind/photovoltaic generating system. *Electric Power Systems Research* 1996;39:35–8.
- [12] Kaabeche A, Belhamel M, Ibtouen R. Sizing optimization of grid-independent hybrid photovoltaic/wind power generation system. *Energy* 2011;36:1214–22.
- [13] Borowy BS, Salameh ZM. Methodology for optimally sizing the combination of a battery bank and PV array in a wind/PV hybrid system. *IEEE Transactions on Energy Conversion* 1996;11:367–75.
- [14] Seeling-Hochmuth GC. A combined optimisation concept for the design and operation strategy of hybrid-PV energy systems. *Solar Energy* 1997;61:77–87.
- [15] Hakimi SM, Moghaddas-Tafreshi SM. Optimal sizing of a stand-alone hybrid power system via particle swarm optimization for Kahnouj area in south-east of Iran. *Renewable Energy* 2009;34:1855–62.
- [16] Ekren O, Ekren BY. Size optimization of a PV/wind hybrid energy conversion system with battery storage using simulated annealing. *Applied Energy* 2010;87:592–8.
- [17] Bernal-Agustín JL, Dufo-López R. Multi-objective design and control of hybrid systems minimizing costs and unmet load. *Electric Power Systems Research* 2009;79:170–80.
- [18] Bernal-Agustín JL, Dufo-López R, Rivas-Ascaso DM. Design of isolated hybrid systems minimizing costs and pollutant emissions. *Renewable Energy* 2006;31:2227–44.
- [19] Dufo-López R, Bernal-Agustín JL. Multi-objective design of PV–wind–diesel–hydrogen–battery systems. *Renewable Energy* 2008;33:2559–72.
- [20] Pelet X, Favrat D, Leyland G. Multiobjective optimisation of integrated energy systems for remote communities considering economics and CO₂ emissions. *International Journal of Thermal Sciences* 2005;44:1180–9.
- [21] Shi J-H, Zhu X-J, Cao G-Y. Design and techno-economical optimization for stand-alone hybrid power systems with multi-objective evolutionary algorithms. *International Journal of Energy Research* 2007;31:315–28.
- [22] Fadaee M, Radzi MAM. Multi-objective optimization of a stand-alone hybrid renewable energy system by using evolutionary algorithms: a review. *Renewable and Sustainable Energy Reviews* 2012;16:3364–9.
- [23] Byrne J, Zhou A, Shen B, Hughes K. Evaluating the potential of small-scale renewable energy options to meet rural livelihoods needs: a GIS- and life-cycle cost-based assessment of Western China's options. *Energy Policy* 2007;35:4391–401.
- [24] Dufo-López R, Bernal-Agustín JL, Yusta-Loyo JM, Domínguez-Navarro JA, Ramírez-Rosado JJ, Lujano J, et al. Multi-objective optimization minimizing cost and life cycle emissions of stand-alone PV–wind–diesel systems with batteries storage. *Applied Energy* 2011;88:4033–41.

- [25] Klucher TM. Evaluation of models to predict insolation on tilted surfaces. *Solar Energy* 1979;23:111–4.
- [26] De Miguel A, Bilbao J, Aguiar R, Kambezidis H, Negro E. Diffuse solar irradiation model evaluation in the North Mediterranean Belt area. *Solar Energy* 2001;70:143–53.
- [27] Durisch W, Bitnar B, Mayor J-C, Kiess H, Lam K, Close J. Efficiency model for photovoltaic modules and demonstration of its application to energy yield estimation. *Solar Energy Materials and Solar Cells* 2007;91:79–84.
- [28] Kasten F, Young AT. Revised optical air mass tables and approximation formula. *Applied Optics* 1989;28:4735–8.
- [29] Notton G, Lazarov V, Stoyanov L. Optimal sizing of a grid-connected PV system for various PV module technologies and inclinations, inverter efficiency characteristics and locations. *Renewable Energy* 2010;35:541–54.
- [30] Thapar V, Agnihotri G, Sethi VK. Critical analysis of methods for mathematical modelling of wind turbines. *Renewable Energy* 2011;36:3166–77.
- [31] Hocaoglu FO, Gerek ON, Kurban M. A novel hybrid (wind–photovoltaic) system sizing procedure. *Solar Energy* 2009;83:2019–28.
- [32] Diaf S, Diaf D, Belhamel M, Haddadi M, Louche A. A methodology for optimal sizing of autonomous hybrid PV/wind system. *Energy Policy* 2007;35:5708–18.
- [33] Piller S, Perrin M, Jossen A. Methods for state-of-charge determination and their applications. *Journal of Power Sources* 2001;96:113–20.
- [34] Downing SD, Socie DF. Simple rainflow counting algorithms. *International Journal of Fatigue* 1982;4:31–40.
- [35] Dufo-López R, Bernal-Agustín JL. Influence of mathematical models in design of PV–diesel systems. *Energy Conversion and Management* 2008;49:820–31.
- [36] Dufo-López R, Bernal-Agustín JL. Design and control strategies of PV–diesel systems using genetic algorithms. *Solar Energy* 2005;79:33–46.
- [37] Dennis Barley C, Byron Winn C. Optimal dispatch strategy in remote hybrid power systems. *Solar Energy* 1996;58:165–79.
- [38] Perera ATD, Wickremasinghe DMJ, Mahindaratna DVS, Attalage RA, Perera KKCK, Bartholameuz EM. Sensitivity of internal combustion generator capacity in standalone hybrid energy systems. *Energy* 2012;39:403–11.
- [39] Diaf S, Notton G, Belhamel M, Haddadi M, Louche A. Design and techno-economical optimization for hybrid PV/wind system under various meteorological conditions. *Applied Energy* 2008;85:968–87.
- [40] Kaldellis JK, Kondili E, Filios A. Sizing a hybrid wind–diesel stand-alone system on the basis of minimum long-term electricity production cost. *Applied Energy* 2006;83:1384–403.
- [41] Kaldellis JK, Zafirakis D, Kavadias K. Minimum cost solution of wind–photovoltaic based stand-alone power systems for remote consumers. *Energy Policy* 2012;42:105–17.
- [42] Yang H, Wei Z, Chengzhi L. Optimal design and techno-economic analysis of a hybrid solar–wind power generation system. *Applied Energy* 2009;86:163–9.
- [43] Shah SD, Cocker III DR, Johnson KC, Lee JM, Soriano BL, Wayne Miller J. Emissions of regulated pollutants from in-use diesel back-up generators. *Atmospheric Environment* 2006;40:4199–209.
- [44] Zhu D, Nussbaum NJ, Kuhns HD, Chang HD, Sodeman D, Uppapalli S. In-plume emission test stand 2: emission factors for 10- to 100-kW U.S. military generators. *Journal of the Air & Waste Management Association* 2009;59:1446.
- [45] Lora EES, Salomon KR. Estimate of ecological efficiency for thermal power plants in Brazil. *Energy Conversion and Management* 2005;46:1293–303.
- [46] Grigg C, Wong P, Albrecht P, Allan R, Bhavaraju M, Billinton R, et al. The IEEE reliability test system-1996. A report prepared by the reliability test system task force of the application of probability methods subcommittee. *IEEE Transactions on Power Systems* 1999;14:1010–20.
- [47] Ashok S. Optimised model for community-based hybrid energy system. *Renewable Energy* 2007;32:1155–64.
- [48] Kaldellis JK, Vlachos GT. Optimum sizing of an autonomous wind–diesel hybrid system for various representative wind-potential cases. *Applied Energy* 2006;83:113–32.
- [49] Li C-H, Zhu X-J, Cao G-Y, Sui S, Hu M-R. Dynamic modeling and sizing optimization of stand-alone photovoltaic power systems using hybrid energy storage technology. *Renewable Energy* 2009;34:815–26.
- [50] Himri Y, Boudghene Stambouli A, Draoui B, Himri S. Techno-economical study of hybrid power system for a remote village in Algeria. *Energy* 2008;33:1128–36.
- [51] Khan MJ, Iqbal MT. Pre-feasibility study of stand-alone hybrid energy systems for applications in Newfoundland. *Renewable Energy* 2005;30:835–54.
- [52] Erdinc O, Uzunoglu M. Optimum design of hybrid renewable energy systems: overview of different approaches. *Renewable and Sustainable Energy Reviews* 2012;16:1412–25.
- [53] Senjyu T, Hayashi D, Yona A, Urasaki N, Funabashi T. Optimal configuration of power generating systems in isolated island with renewable energy. *Renewable Energy* 2007;32:1917–33.
- [54] Moghaddas-Tafreshi SM, Zamani HA, Hakimi SM. Optimal sizing of distributed resources in micro grid with loss of power supply probability technology by using breeding particle swarm optimization. *Journal of Renewable and Sustainable Energy* 2011;3:043105. 17.
- [55] Deb K, Mohan M, Mishra S. Evaluating the ϵ -domination based multi-objective evolutionary algorithm for a quick computation of Pareto-optimal solutions. *Evolutionary Computation* 2005;13:501–25.
- [56] Laumanns M, Thiele L, Deb K, Zitzler E. Combining convergence and diversity in evolutionary multiobjective optimization. *Evolutionary Computation* 2002;10:263–82.
- [57] Deb K, Beyer H. Self-adaptive genetic algorithms with simulated binary crossover. *Complex Systems* 1999;9:431–54.
- [58] Deb K. An efficient constraint handling method for genetic algorithms. *Computer Methods in Applied Mechanics and Engineering* 2000;186:311–38.
- [59] Bolinger M, Wiser R. Understanding wind turbine price trends in the U.S. over the past decade. *Energy Policy* 2012;42:628–41.
- [60] <http://www.solarbuzz.com/facts-and-figures/retail-price-environment/solar-electricity-prices> [accessed 15.08.2012].